

Chapter 7

Spin-Dependent Transport of Carbon Nanotubes with Chromium Atoms

S.P. Kruchinin, S.P. Repetsky, and I.G. Vyshyvana

Abstract This paper presents a new method of describing electronic correlations in disordered magnetic crystals based on the Hamiltonian of multi-electron system and diagram method for Green's functions finding. Electronic states of a system were approximately described by self-consistent multi-band tight-binding model. The Hamiltonian of a system is defined on the basis of Kohn–Sham orbitals. Potentials of neutral atoms are defined by the meta-generalized gradient approximation (MGGA). Electrons scattering on the oscillations of the crystal lattice are taken into account. The proposed method includes long-range Coulomb interaction of electrons at different sites of the lattice. Precise expressions for Green's functions, thermodynamic potential and conductivity tensor are derived using diagram method. Cluster expansion is obtained for density of states, free energy, and electrical conductivity of disordered systems. We show that contribution of the electron scattering processes to cluster expansion is decreasing along with increasing number of sites in the cluster, which depends on small parameter. The computation accuracy is determined by renormalization precision of the vertex parts of the mass operators of electron-electron and electron-phonon interactions. This accuracy also can be determined by small parameter of cluster expansion for Green's functions of electrons and phonons. It was found the nature of spin-dependent electron transport in carbon nanotubes with chromium atoms, which are adsorbed on the surface. We show that the phenomenon of spin-dependent electron transport in a carbon nanotube was the result of strong electron correlations, caused by the presence of chromium atoms. The value of the spin polarization of electron transport is determined by the difference of the partial densities of electron states with opposite spin projection at the Fermi level. It is also determined by the difference between the relaxation times arising from different occupation numbers of single-electron states of carbon

S.P. Kruchinin
Bogolyubov Institute for Theoretical Physics, Kiev, 03680, Ukraine

S.P. Repetsky (✉)
Taras Shevchenko Kiev National University, Vladimirskaya st., 64, Kiev, 01033, Ukraine
e-mail: srepetsky@univ.kiev.ua

I.G. Vyshyvana
Institute of High Technologies, Taras Shevchenko Kiev National University, Akademika
Glushkova avenue, 4g, Kiev, 02033, Ukraine

© Springer Science+Business Media Dordrecht 2016
J. Bonča, S. Kruchinin (eds.), *Nanomaterials for Security*, NATO Science for Peace
and Security Series A: Chemistry and Biology, DOI 10.1007/978-94-017-7593-9_7

67

and chromium atoms. The value of the electric current spin polarization increases along with Cr atoms concentration and magnitude of the external magnetic field increase.

7.1 Introduction

The progress of describing disordered systems is connected with the development of electron theory. Substitution alloys are best described among disordered systems. The traditional knowledge about physical properties of alloys is based on Born approximation in the scattering theory. However, this approach obviously can not be applied in the case of large scattering of potential difference of components which are held for the description of alloys with simple transition and rare-earth elements. The same difficulty is typical for the pseudopotential method [8]. Because of the pseudopotentials non-local nature there is a problem of their transferability. It is impossible to use nuclear potentials determined by the properties of some systems to describe other systems. Significant success in the study of the electronic structure and properties of the systems was achieved recently due to use of the ultrasoft Vanderbilt's pseudopotential [21, 37] and the method of projector-augmented waves in density functional theory proposed by Blohl [2, 16]. This approach was developed further thanks to generalized gradient approximation (GGA) usage in density functional theory of multi-electron systems developed by Perdew in his papers [23–25, 35, 36]. The wave function of the valence states of electron (all-electron orbital) is denoted in projector-augmented waves approach by using the conversion through the pseudo-orbital. The pseudo-orbital waves expand to pseudo partial ones in the augment area. Even so, the all-electron orbital in the same area are expanded with the same coefficients via partial waves that are described by Kohn–Sham equation. The expression for the Hamiltonian operator, which we have in equation for pseudo wave function, is derived by minimizing the full energy functional. Using this equation, and expanding pseudo orbital by plane waves, we can derive the set of equations for expansion coefficients. From this system it is possible to get the electron energetic spectrum, wave functions, and the value of the full energy functional. The method for describing the electron structure of crystals is shown in Ref. [35], using VASP program package. With the help of the cluster methods of calculation and the GAUSSIAN program package, this approach could be used for molecule electronic structure description.

It should be noted that recently in papers (e.g. Refs. [6, 7, 9–11, 14, 26, 35]), the simple effective calculation method of electronic structure and properties for big molecules have been proposed. This method is based on the tight-binding model and functional density theory, which includes long-range coulomb interaction of electrons on different sites of crystal lattice. The long-range coulomb interaction of electrons on different sites is described in the local density approximation.

However, mentioned methods [6, 7, 9–11, 14, 23–26, 35, 36] are used only for an ideal ordered crystals and molecules description. In disordered crystals, the effects

associated with localized electronic states and lattice vibrations are arise. They can not be described in the model of ideal crystal. In this regard, other approaches are also developed.

Essential achievements in description of the disordered systems properties are connected with application of the tight-binding model in the multi-scattering theory, including approximation of the coherent potential. Starting from Slater's and Koster's work [29, 31] tight-binding model in description of the ideal crystals properties were frequently applied. Later it was generalized for the case of disordered systems.

The method of describing magnetic alloys electronic structure, based on the functional density theory, was proposed by Staunton et al. [32] and Razee et al. [27]. The effective potential in Kohn–Sham equation [13, 15] consists of atomic potential and Pauli's addition, which is expressed through the magnetic field induction. Atomic potential and the magnetic field induction are expressed through variational derivatives of exchange-correlation energy by electronic density and magnetization respectively. Calculations of the electronic structure of the magnetic alloy are based on the mentioned effective potentials and usage of the self-consistent Korringa–Kohn–Rostoker coherent potential approximation. It was more developed in further papers [12, 33, 34]. The method of interatomic pair correlations parameter calculation was proposed by Staunton et al. [32] due to the pair mixing potential, which is expressed through the second derivative of the thermodynamic potential of the alloy concentration [3]. This thermodynamic potential is calculated in the one site coherent potential approximation. It should be noted that the methods developed in papers [12, 29, 31–34] do not include long-range Coulomb interaction of electrons at different lattice sites.

In our work a new method of describing electronic correlations in disordered magnetic crystals based on the Hamiltonian of multi-electron system and the diagram method for finding Green's functions was developed. Electronic correlations in crystals were described in self-consistent multi-band tight-binding model. The wave functions of non-interacting atoms are calculated based upon the Kohn–Sham equation. The effective one-electron potential of the many-atom structure is approximated as a sum of spherical Kohn–Sham potential of neutral non-interacting atoms. Potential of neutral atoms are defined by the meta-generalized gradient approximation (MGGA) [24, 35]. Our model includes wave functions and atomic potentials recalculation, taking into account the electronic density redistribution as the result of atomic interaction. It is also includes long-range Coulomb interaction of the electrons on different sites of the crystal lattice. Electron scattering processes on the ionic core potentials of different sorts and on oscillations of crystal lattice are considered. The two-time Green's function calculations are based on the temperature Green's function [22, 28]. In this operation a known relation between spectral representation for two-time and temperature Green's function was used [1].

Calculation of two-time Green's function of the disordered crystal are based on diagram technique, analogous to diagram technique for homogeneous system [1]. The set of equations for two-time Green's function, expressions for free energy and electrical conductivity of disordered crystals are derived. Calculation accuracy of

the energetic spectrum, free energy, and electrical conductivity are determined by accuracy of the electron-electron and electron-phonon mass operators vertex parts renormalization. Energetic spectrum, free energy, conductivity and spin-depended transport of nanotubes doped with Cr atoms calculations are based on this method.

7.2 Hamiltonian of Electron's and Phonon's System for Disordered Crystals

Hamiltonian of the disordered crystal consists of single-particle Hamiltonian of electrons in the ionic cores field, the potential energy of the pair electron-electron interaction, lattice oscillations Hamiltonian and Hamiltonian of electron-phonon interaction.

Hamiltonian of the disordered crystal is represented on the basis of wave functions for free neutral atoms. In the Wannier representation the system Hamiltonian is, [28]

$$H = H_0 + H_{\text{int}}, \quad (7.1)$$

where zero-order Hamiltonian

$$H_0 = H_e^{(0)} + H_{ph}^{(0)}, \quad (7.2)$$

consists from single-particle Hamiltonian of electrons in the ionic cores field

$$H_e^{(0)} = \sum_{\substack{n_1 i_1 \gamma_1 \\ n_2 i_2 \gamma_2}} h_{n_1 i_1 \gamma_1, n_2 i_2 \gamma_2}^{(0)} a_{n_1 i_1 \gamma_1}^+ a_{n_2 i_2 \gamma_2} \quad (7.3)$$

and atomic nucleus Hamiltonian

$$H_{ph}^{(0)} = \sum_{ni\alpha} \frac{P_{ni\alpha}^2}{2M_i} + \frac{1}{2} \sum_{\substack{n_1 i_1 \alpha_1 \\ n_2 i_2 \alpha_2}} \Phi_{n_1 i_1 \alpha_1, n_2 i_2 \alpha_2}^{(0)} u_{n_1 i_1 \alpha_1} u_{n_2 i_2 \alpha_2}. \quad (7.4)$$

Here in Eq. (7.3), (7.4) different sort ion cores distribution on sites (ni) of crystal lattice is the same as for ideally ordered crystal.

Perturbation Hamiltonian in Eq.(7.1) is

$$H_{\text{int}} = \delta\Phi + H_{ei} + H_{eph} + H_{ee} + H_{phi} + H_{phph}. \quad (7.5)$$

Perturbation Hamiltonian H_{int} consists of different sorts ion core interaction energy $\delta\Phi$. Interaction energy $\delta\Phi$ is measured from energy level for ideally ordered crystal. Addition to single-particle Hamiltonian of electrons in the ionic cores field in Eq. (7.3) (electron-ion interaction Hamiltonian) is defined as

$$H_{ei} = \sum_{\substack{n_1 i_1 \gamma_1 \\ n_2 i_2 \gamma_2}} w_{n_1 i_1 \gamma_1, n_2 i_2 \gamma_2} a_{n_1 i_1 \gamma_1}^+ a_{n_2 i_2 \gamma_2}. \quad (7.6)$$

Hamiltonian of electron's interaction with oscillations of the crystal lattice (named as electron-phonon interaction) is defined as

$$H_{eph} = \sum_{\substack{n_1 i_1 \gamma_1 \\ n_2 i_2 \gamma_2}} v'_{n_1 i_1 \gamma_1, n_2 i_2 \gamma_2} a_{n_1 i_1 \gamma_1}^+ a_{n_2 i_2 \gamma_2}. \quad (7.7)$$

Electron-electron pair interaction Hamiltonian is

$$H_{ee} = \frac{1}{2} \sum_{\substack{n_1 i_1 \gamma_1 \\ n_2 i_2 \gamma_2 \\ n_3 i_3 \gamma_3 \\ n_4 i_4 \gamma_4}} v_{n_3 i_3 \gamma_3, n_4 i_4 \gamma_4}^{(2) n_1 i_1 \gamma_1, n_2 i_2 \gamma_2} a_{n_1 i_1 \gamma_1}^+ a_{n_2 i_2 \gamma_2}^+ a_{n_3 i_3 \gamma_3} a_{n_4 i_4 \gamma_4}. \quad (7.8)$$

Atomic nucleus Hamiltonian component, caused by disordered distribution of atoms (phonon-impurity interaction Hamiltonian) is defined as

$$H_{phi} = \frac{1}{2} \sum_{\substack{n_1 i_1 \alpha_1 \\ n_2 i_2 \alpha_2}} \Delta M_{n_1 i_1 \alpha_1, n_2 i_2 \alpha_2}^{-1} P_{n_1 i_1 \alpha_1} P_{n_2 i_2 \alpha_2} \\ + \frac{1}{2} \sum_{\substack{n_1 i_1 \alpha_1 \\ n_2 i_2 \alpha_2}} \Delta \Phi_{n_1 i_1 \alpha_1, n_2 i_2 \alpha_2} u_{n_1 i_1 \alpha_1} u_{n_2 i_2 \alpha_2}, \quad (7.9)$$

where

$$\Delta M_{n_1 i_1 \alpha_1, n_2 i_2 \alpha_2}^{-1} = \left(\frac{1}{M_{n_1 i_1}} - \frac{1}{M_{i_1}} \right) \delta_{n_1 n_2} \delta_{i_1 i_2} \delta_{\alpha_1 \alpha_2},$$

$\Delta \Phi_{n_1 i_1 \alpha_1, n_2 i_2 \alpha_2} = \Phi_{n_1 i_1 \alpha_1, n_2 i_2 \alpha_2} - \Phi_{n_1 i_1 \alpha_1, n_2 i_2 \alpha_2}^{(0)}$, $M_{n_1 i_1}$, M_{i_1} – mass of the atom in the site (ni) for disordered and ordered alloy accordingly.

The anharmonic component of atomic nucleus Hamiltonian (phonon-phonon interaction Hamiltonian) is

$$H_{phph} = \frac{1}{3!} \sum_{\substack{n_1 i_1 \alpha_1 \\ n_2 i_2 \alpha_2 \\ n_3 i_3 \alpha_3}} \Phi_{n_1 i_1 \alpha_1, n_2 i_2 \alpha_2, n_3 i_3 \alpha_3}^{(0)} u_{n_1 i_1 \alpha_1} u_{n_2 i_2 \alpha_2} u_{n_3 i_3 \alpha_3}. \quad (7.10)$$

In Eq. (7.10) only anharmonic terms of third order are taken into account.

In the previously written expressions $a_{ni\gamma}^+$, $a_{ni\gamma}$ are creation and destruction operators in the state, described by Wannier function $\phi_{ni\gamma}(\xi) = \langle \xi | ni\gamma \rangle$, where $\xi = (\mathbf{r}, \sigma)$. In these notations state's index γ includes as quantum number $\sigma = 1/2, -1/2$ which defines the value of spin projection on z axis and a set of other quantum numbers which describes electron spatial movements. Here n is the number of primitive cell, i – sublattice site number in primitive cell, \mathbf{r} is electron's radius-vector, u_{ni} – atoms displacement operator in site (ni); $P_{ni\alpha}$ – operator of α -projection of atom's momentum on orthogonal axes.

The wave functions of an electron in free neutral atom sort λ , which is located at the site (ni), are obtained from Kohn–Sham equation in density functional theory [25, 26]:

$$\left[-\frac{\hbar^2}{2m} \nabla^2 + V_{ext}^\lambda(\mathbf{r}) + V_H^{\lambda i}(\mathbf{r}) + V_{XC,\sigma}^{\lambda i}(\mathbf{r}) \right] \times \psi_{i\delta\sigma}^\lambda(\mathbf{r}) = \varepsilon_{i\delta\sigma}^\lambda \psi_{i\delta\sigma}^\lambda(\mathbf{r}), \quad (7.11)$$

where σ is quantum number of spin projection on axis z ; $\delta = (\tilde{\varepsilon}lm)$, l, m are quantum numbers of angular momentum and $\tilde{\varepsilon}$ is quantum number that describes the value of electron energy. To reduce the length of Eq. (7.11) $(\mathbf{r} - \mathbf{r}_{ni})$ is denoted by (\mathbf{r}) .

In expression (7.11) the value $V_{ext}^\lambda(\mathbf{r})$ is potential energy of an electron in the atom's core field of sort λ at the site (n),

$$V_H^{\lambda i}(\mathbf{r}) = \int dv' \frac{e^2}{|\mathbf{r} - \mathbf{r}'|} n_{\lambda i}(\mathbf{r}') \quad (7.12)$$

– the Hartree potential.

In Eq. (7.12) electron density is

$$n_{\lambda i}(\mathbf{r}) = n_{\lambda i\sigma}(\mathbf{r}) + n_{\lambda i-\sigma}(\mathbf{r}). \quad (7.13)$$

The electron density with projection of spin σ is given by expression

$$n_{\lambda i\sigma}(\mathbf{r}) = \sum_{\delta} Z_{i\delta\sigma}^\lambda \psi_{i\delta\sigma}^\lambda *_{i\delta\sigma}(\mathbf{r}) \psi_{i\delta\sigma}^\lambda(\mathbf{r}), \quad (7.14)$$

where $Z_{i\delta\sigma}^\lambda$ – occupation number of electron state ($i\delta\sigma$), assuming that an atom of sort λ is in the site (ni).

In MGGA obtained by Perdew [24, 35] and based on density functional theory, the exchange-correlation potential $V_{XC,\sigma}(\mathbf{r}) = V_{XC,\sigma}^{\text{MGGA}}(\mathbf{r})$ can be represented as:

$$V_{XC,\sigma}^{\text{MGGA}}(\mathbf{r}) \psi_{\gamma\sigma}(\mathbf{r}) = V_{XC,\sigma}^{\text{GGA}}(r) \psi_{\gamma\sigma}(\mathbf{r}) - \frac{1}{2} \nabla \cdot \{ \mu_{XC,\sigma}(r) \nabla \} \psi_{\gamma\sigma}(\mathbf{r}), \quad (7.15)$$

where

$$V_{XC,\sigma}^{\text{GGA}}(r) = \left[\frac{\partial e_{XC}^{\text{MGGA}}}{\partial n_\sigma} - \nabla \cdot \left(\frac{\partial e_{XC}^{\text{MGGA}}}{\partial \nabla n_\sigma} \right) \right], \quad \mu_{XC,\sigma}(r) = \frac{\partial e_{XC}^{\text{MGGA}}}{\partial \tau_\sigma},$$

$e_{XC}^{\text{MGGA}}(2n_\sigma)/2$ is exchange-correlational energy density, $\tau_\sigma = \sum_\delta |\nabla \psi_{\delta\sigma}|^2 / 2$ is kinetic energy density.

Wave functions of the basis set $\phi_{ni\gamma\sigma}(\mathbf{r})$, on which Hamiltonian of the system is represented as in Eq. (7.1), are defined from Kohn–Sham Eq. (7.11) for atom of sort λ_i and equals to $\phi_{ni\gamma\sigma}(\mathbf{r}) = R_{i\tilde{e}l\sigma}^{\lambda_i}(|\mathbf{r} - \mathbf{r}_{ni}|) Y_{lm}^v(\theta, \phi)$, where $R_{i\tilde{e}l\sigma}^{\lambda_i}(|\mathbf{r} - \mathbf{r}_{ni}|)$ – radial part of wave function in Eq. (7.11), λ_i – sort of atom which located in site (ni) of ideal ordered crystal. Real spherical functions $Y_{lm}^v(\theta, \phi)$, are related with complex spherical functions $Y_{lm}(\theta, \phi)$ by equations

$$\begin{aligned} Y_{lm}^c(\theta, \phi) &= \frac{1}{\sqrt{2}} [Y_{lm}(\theta, \phi) + Y_{lm}^*(\theta, \phi)], \\ Y_{lm}^s(\theta, \phi) &= \frac{1}{i\sqrt{2}} [Y_{lm}(\theta, \phi) - Y_{lm}^*(\theta, \phi)], \quad m \neq 0. \end{aligned} \quad (7.16)$$

The potential energy operator of electron in the field of different sort ionic cores can be expressed

$$V(\mathbf{r}) = \sum_{ni} v^{ni}(\mathbf{r} - \mathbf{r}'_{ni}), \quad \mathbf{r}'_{ni} = \mathbf{r}_{ni} + \mathbf{u}_{ni}^s + \mathbf{u}_{ni},$$

where \mathbf{r} – electron's radius vector, $\mathbf{r}_{ni} = \mathbf{r}_n + \boldsymbol{\rho}_i$ – radius-vector of atom's equilibrium position in site of crystal lattice (ni), \mathbf{u}_{ni}^s – is vector of atom's static displacement from equilibrium position in site (ni).

Potentials of ionic core $v^{\lambda_i}(\mathbf{r} - \mathbf{r}_{ni})$ are found from Eqs. (7.11), (7.12), (7.13), (7.14) and (7.15). While finding potentials $v^{\lambda_i}(\mathbf{r} - \mathbf{r}_{ni})$ summation in Eq. (7.14) must be done by electronic states of ionic cores.

Values $h_{n_1 i_1 \gamma_1, n_2 i_2 \gamma_2}^{(0)}$ in Eq. (7.3) are the matrix elements of the kinetic and potential $\sum_{ni} v^{\lambda_i}(\mathbf{r} - \mathbf{r}_{ni})$ energy operators of electron in the field of ionic core, where λ_i – sort of ion which located in site (ni) of ideal ordered crystal. Matrix elements are calculated by Slater–Koster method [11, 35].

Matrix element of electron-ion interaction Hamiltonian in Eq. (7.6) is

$$w_{n_1 i_1 \gamma_1, n_2 i_2 \gamma_2} = \sum_{ni} w_{n_1 i_1 \gamma_1, n_2 i_2 \gamma_2}^{ni}, \quad (7.17)$$

where

$$w_{n_1 i_1 \gamma_1, n_2 i_2 \gamma_2}^{ni} = \sum_{\lambda} c_{ni}^{\lambda} w_{n_1 i_1 \gamma_1, n_2 i_2 \gamma_2}^{\lambda ni},$$

$$w_{n_1 i_1 \gamma_1, n_2 i_2 \gamma_2}^{\lambda ni} = v_{n_1 i_1 \gamma_1, n_2 i_2 \gamma_2}^{\lambda ni} + \Delta v_{n_1 i_1 \gamma_1, n_2 i_2 \gamma_2}^{\lambda ni} - v_{n_1 i_1 \gamma_1, n_2 i_2 \gamma_2}^{\lambda_i ni},$$

λ_i is sort of ion which located in site (ni) of ideal ordered crystal. Here c_{ni}^{λ} – random numbers, taking value 1 or 0 depending on whether the atom of sort λ is at site (ni) or not.

Hamiltonian of electron-phonon interaction defined in Eq. (7.7) is expressed through derivatives of potential energy of electron in ions core field by projections of displacement vector \mathbf{u}_{ni} of atom. In Eq. (7.7) the value of $v'_{n_1 i_1 \gamma_1, n_2 i_2 \gamma_2}$ is given by $v'_{n_1 i_1 \gamma_1, n_2 i_2 \gamma_2} = \sum_{ni\alpha} v_{n_1 i_1 \gamma_1, n_2 i_2 \gamma_2}^{ni\alpha} u_{ni\alpha}$, where $v_{n_1 i_1 \gamma_1, n_2 i_2 \gamma_2}^{ni\alpha} = \sum_{\lambda} c_{ni}^{\lambda} v'_{n_1 i_1 \gamma_1, n_2 i_2 \gamma_2}^{\lambda ni\alpha}$. Value $v'_{n_1 i_1 \gamma_1, n_2 i_2 \gamma_2}^{\lambda ni\alpha}$ is matrix element of operator $-e_{ni\alpha} \frac{d}{d|\mathbf{r}-\mathbf{r}_{ni}|} v^{\lambda} (|\mathbf{r}-\mathbf{r}_{ni}|)$, where $e_{ni} = \frac{\mathbf{r}-\mathbf{r}_{ni}}{|\mathbf{r}-\mathbf{r}_{ni}|}$.

Values $\Delta v_{n_1 i_1 \gamma_1, n_2 i_2 \gamma_2}^{\lambda ni}$ in Eq. (7.17) describe electron scattering on static displacement of atoms and defined by equation

$$\Delta v_{n_1 i_1 \gamma_1, n_2 i_2 \gamma_2}^{\lambda ni} = \sum_{\alpha} v'_{n_1 i_1 \gamma_1, n_2 i_2 \gamma_2}^{\lambda ni\alpha} u_{ni\alpha}^s.$$

The matrix of force constant part which is caused by the direct coulomb interaction of ionic cores has the form:

$$\Phi_{ni\alpha, n'i'\alpha'} = -\frac{Z_{ni} Z_{n'i'} e^2}{4\pi \epsilon_0 |\mathbf{r}_n + \boldsymbol{\rho}_i - \mathbf{r}_{n'} - \boldsymbol{\rho}_{i'}|^5}$$

$$\times \left[3 (r_{n\alpha} + \rho_{i\alpha} - r_{n'\alpha} - \rho_{i'\alpha}) (r_{n\alpha'} + \rho_{i\alpha'} - r_{n'\alpha'} - \rho_{i'\alpha'}) \right.$$

$$\left. - |\mathbf{r}_n + \boldsymbol{\rho}_i - \mathbf{r}_{n'} - \boldsymbol{\rho}_{i'}|^2 \delta_{\alpha\alpha'} \right], \quad (ni) \neq (n'i'), \quad (7.18)$$

where Z_{ni} – valence of ion cores which located in the site (ni).

Diagonal by number site (ni) elements of the matrix of force constants is determined from the condition:

$$\sum_{n'i'} \Phi_{ni\alpha, n'i'\alpha'} = 0.$$

Values $\Phi_{n_1 i_1 \alpha_1, n_2 i_2 \alpha_2}^{(0)}$, $\Phi_{n_1 i_1 \alpha_1, n_2 i_2 \alpha_2, n_3 i_3 \alpha_3}^{(0)}$ in Eq. (7.4), (7.10) are force constants.

Matrix $\Phi_{n i \alpha, n' i' \alpha'}^{(0)}$ is derived from expression for matrix $\Phi_{n i \alpha, n' i' \alpha'}$ in which $Z_{ni} = Z^{\lambda_i}$, where Z^{λ_i} is valence of ion which is located in the site (ni) of ideal ordered crystal.

Matrix elements $v_{n_3 i_3 \gamma_3, n_4 i_4 \gamma_4}^{(7.2) n_1 i_1 \gamma_1, n_2 i_2 \gamma_2}$ of Hamiltonian in Eq. (7.8) can be calculated by integrating angular variables. Integrals from product of three spherical functions (Gaunt integral) can be represented using the Clebsch–Gordan coefficients [31]. As a result matrix elements $v_{\tilde{\varepsilon}_3 l_3 m_3, \tilde{\varepsilon}_4 l_4 m_4}^{(2) \tilde{\varepsilon}_1 l_1 m_1, \tilde{\varepsilon}_2 l_2 m_2}$ are obtained:

$$\begin{aligned}
v_{\tilde{\varepsilon}_1 l_1 m_1, \tilde{\varepsilon}' l' m'}^{(2) \tilde{\varepsilon} l m, \tilde{\varepsilon}_2 l_2 m_2} &= e^2 \sum_{\substack{|l-l'| \leq l_3 \leq l+l' \\ |l_2-l_1| \leq l_3 \leq l_2+l_1 \\ l+l'+l_3 = 2k, k_1 \in \mathbb{N} \\ l_2+l_1+l_3 = 2k_1, k_1 \in \mathbb{N}}} \frac{1}{2l_3+1} \\
&\times \left[\frac{(2l_3+1)(2l'+1)(2l_3+1)(2l_1+1)}{(2l+1)(2l_2+1)} \right]^{1/2} \\
&\times c(l_3 l' l; 0, 0) c(l_3 l' l; m', m') c(l_3 l_1 l_2; 0, 0) c(l_3 l_1 l_2; m_2 - m_1, m_1) \\
&\times \left[\int_0^\infty dr_1 r_1^2 R_{\tilde{\varepsilon} l}(r_1) R_{\tilde{\varepsilon}' l'}(r_1) \int_0^{r_1} dr_2 r_2^2 R_{\tilde{\varepsilon}_2 l_2}(r_2) R_{\tilde{\varepsilon}_1 l_1}(r_2) \frac{r_2^{l_3}}{r_1^{l_3+1}} \right. \\
&\left. + \int_0^\infty dr_2 r_2^2 R_{\tilde{\varepsilon}_2 l_2}(r_2) R_{\tilde{\varepsilon}_1 l_1}(r_2) \int_0^{r_2} dr_1 r_1^2 R_{\tilde{\varepsilon} l}(r_1) R_{\tilde{\varepsilon}' l'}(r_1) \frac{r_1^{l_3}}{r_2^{l_3+1}} \right], \quad (7.19)
\end{aligned}$$

where l, m are orbital and magnetic quantum numbers, respectively, $c(l'' l' l; m'', m')$ – Clebsch–Gordan coefficients [31], $R_{\tilde{\varepsilon} l}(r)$ – radial part of wave function, $\tilde{\varepsilon}$ – main quantum number.

Matrix elements on the basis of real wave functions [35] $v_{n_3 i_3 \gamma_3, n_4 i_4 \gamma_4}^{(2) n_1 i_1 \gamma_1, n_2 i_2 \gamma_2}$ for each site when $(n_1, i_1) = (n_2, i_2) = (n_3, i_3) = (n_4, i_4)$ are expressed by linear combinations of matrix elements $v_{\tilde{\varepsilon}_3 l_3 m_3, \tilde{\varepsilon}_4 l_4 m_4}^{(2) \tilde{\varepsilon}_1 l_1 m_1, \tilde{\varepsilon}_2 l_2 m_2}$. This procedure of matrix elements calculation can be easily programmed.

Matrix elements on the basis of real wave functions $v_{n_3 i_3 \gamma_3, n_4 i_4 \gamma_4}^{(2) n_1 i_1 \gamma_1, n_2 i_2 \gamma_2}$ for different sites (ni) can be approximately represented in the form similar to formula (7.19), if we describe radial part of the wave function by Gaussian function (namely Gaussian orbital), as this is done in the method of molecular orbitals – linear combinations of atomic orbitals [29]. In this approximation the multi-center integrals $v_{n_3 i_3 \gamma_3, n_4 i_4 \gamma_4}^{(2) n_1 i_1 \gamma_1, n_2 i_2 \gamma_2}$ have the form of one-center integrals, as the product of two Gaussian orbitals that are localized at different centers can be reduced to the product of orbitals that are localized at the joint center.

7.3 Green's Functions of Electrons and Phonons System

In order to calculate the energy spectrum of electrons and phonons, free energy and electrical conductivity of disordered crystal we introduce two-time Green's function. We define two-time retarded $G_r^{AB}(t, t')$ and accelerated $G_a^{AB}(t, t')$ Green's functions as follows[41]:

$$\begin{aligned} G_r^{AB}(t, t') &= -\frac{i}{\hbar}\theta(t-t')\langle[\tilde{A}(t), \tilde{B}(t')]\rangle, \\ G_a^{AB}(t, t') &= \frac{i}{\hbar}\theta(t'-t)\langle[\tilde{A}(t), \tilde{B}(t')]\rangle. \end{aligned} \quad (7.20)$$

Operator in the Heisenberg representation reads

$$\tilde{A}(t) = e^{iHt/\hbar} A e^{-iHt/\hbar},$$

where \hbar – Planck's constant, $H = H - \mu_e N_e$, μ_e is chemical potential of electron subsystem and N_e is the operator of electrons number:

$$N_e = \sum_{ni\gamma} a_{ni\gamma}^+ a_{ni\gamma}.$$

In Eq. (7.20)

$$[A, B] = AB - \eta BA, \quad (7.21)$$

where for Bose operators A, B $\eta = 1$ and for Fermi operators $\eta = -1$, $\theta(t)$ is Heaviside's step function.

Brackets $\langle \dots \rangle$ in Eq. (7.20) denote averaging

$$\langle A \rangle = \text{Sp}(\rho A), \quad \rho = e^{(\Omega - H)/\Theta}, \quad (7.22)$$

where Ω is thermodynamic potential of the system, $\Theta = k_b T$, T – temperature.

Calculation of two-time retarded and accelerated Green's functions defined in Eq. (7.20) is based on the calculation of temperature Green's functions. Known relation between the spectral representation for retarded, accelerated and temperature Green's functions is used.

The temperature Green's function defined as

$$G^{AB}(\tau, \tau') = -\langle T_\tau \tilde{A}(\tau) \tilde{B}(\tau') \rangle, \quad (7.23)$$

where operator $\tilde{A}(\tau)$ is derived from $\tilde{A}(t)$ in Eq. (7.20) by replacing $t = -i\hbar\tau$,

$$\begin{aligned}\tilde{A}(\tau) &= e^{H\tau} A e^{-H\tau}, \\ T_\tau \tilde{A}(\tau) \tilde{B}(\tau') &= \theta(\tau - \tau') \tilde{A}(\tau) \tilde{B}(\tau') + \eta \theta(\tau' - \tau) \tilde{B}(\tau') \tilde{A}(\tau),\end{aligned}$$

here for Bose operators A, B $\eta = 1$ and for Fermi operators $\eta = -1$.

We introduce the operator

$$\sigma(\tau) = e^{H_0\tau} e^{-H\tau}, \quad (7.24)$$

where $H = H_0 + H_{\text{int}}$, $H_0 = H_0 - \mu_e N_e$.

Differentiating the expression $\sigma(\tau)$ in Eq. (7.24) by τ parameter and consequently integrating by the condition $\sigma(0) = 1$, we obtain:

$$\sigma(\tau) = T_\tau \exp \left[- \int_0^\tau H_{\text{int}}(\tau') d\tau' \right], \quad (7.25)$$

where $H_{\text{int}}(\tau) = e^{H_0\tau} H_{\text{int}} e^{-H_0\tau}$.

Taking into account expression (7.24) we can write

$$\tilde{A}(\tau) = \sigma^{-1}(\tau) A(\tau) \sigma(\tau). \quad (7.26)$$

Taking to account Eqs. (7.25), (7.26) for temperature Green's function in Eq. (7.23) we can obtain equation

$$G^{AB}(\tau, \tau') = - \frac{\langle T_\tau A(\tau) B(\tau') \sigma(1/\Theta) \rangle_0}{\langle \sigma(1/\Theta) \rangle_0} \quad (7.27)$$

where

$$\langle A \rangle_0 = \text{Sp}(\rho_0 A), \quad \rho_0 = e^{(\Omega_0 - H_0)/\Theta}.$$

Expanding the exponent $\sigma(\tau)$ in expression (7.25) in a series of powers $H_{\text{int}}(\tau)$, substituting the result in Eq. (7.27) and using Wick's theorem for calculating the temperature Green's functions of disordered crystals [28] it is possible to build a diagram technique similar to a homogeneous system [1]. The denominator in Eq. (7.27) reduces from the same factor in the numerator. So Green's function can be expressed in a series only connected diagrams. Using the relation between the spectral representations of temperature and time Green's functions [1], by analytic continuation to real axis we obtain the following system of equations for retarded Green functions (hereinafter index r will be omitted) [28]:

$$\begin{aligned}G^{aa^+}(\varepsilon) &= G_0^{aa^+}(\varepsilon) + G_0^{aa^+}(\varepsilon) (w + \Sigma_{eph}(\varepsilon) + \Sigma_{ee}(\varepsilon)) G^{aa^+}(\varepsilon) \\ &\times G^{uu}(\varepsilon) = G_0^{uu}(\varepsilon) + G_0^{uu}(\varepsilon) (\Delta\Phi + \Sigma_{phe}(\varepsilon) + \Sigma_{phph}(\varepsilon)) \\ &\times G^{uu}(\varepsilon) + G_0^{uP}(\varepsilon) \Delta M^{-1} G^{Pu}(\varepsilon),\end{aligned}$$

$$\begin{aligned}
G^{PP}(\varepsilon) &= G_0^{PP}(\varepsilon)G_0^{PP}(\varepsilon)\Delta M^{-1}G^{PP}(\varepsilon) + G_0^{Pu}(\varepsilon) \\
&\quad \times (\Delta\Phi + \Sigma_{phe}(\varepsilon) + \Sigma_{phph}(\varepsilon))G^{uP}(\varepsilon), \\
G^{uP}(\varepsilon) &= G_0^{uP}(\varepsilon) + G_0^{uP}(\varepsilon)\Delta M^{-1}G^{PP}(\varepsilon) + G_0^{uu}(\varepsilon) \\
&\quad \times (\Delta\Phi + \Sigma_{phe}(\varepsilon) + \Sigma_{phph}(\varepsilon))G^{uP}(\varepsilon), \\
G^{Pu}(\varepsilon) &= G_0^{Pu}(\varepsilon) + G_0^{Pu}(\varepsilon)(\Delta\Phi + \Sigma_{phe}(\varepsilon) + \Sigma_{phph}(\varepsilon)) \\
&\quad \times G^{uu}(\varepsilon) + G_0^{PP}(\varepsilon)\Delta M^{-1}G^{Pu}(\varepsilon), \tag{7.28}
\end{aligned}$$

where $\varepsilon = \hbar\omega$.

Here $G^{aa^\dagger}(\varepsilon)$, $G^{uu}(\varepsilon)$, $G^{PP}(\varepsilon)$, $G^{uP}(\varepsilon)$, $G^{Pu}(\varepsilon)$ are spectral representation of one-particle Green's function of the electrons subsystem and Green's functions "shift-shift", "impulse-impulse", "shift-impulse" "impulse-shift" of phonons subsystem; $\Sigma_{eph}(\varepsilon)$, $\Sigma_{phe}(\varepsilon)$, $\Sigma_{ee}(\varepsilon)$, $\Sigma_{phph}(\varepsilon)$ – actual energetic parts (mass operators) which describe the electron-phonon, phonon-electron, electron-electron and phonon-phonon interactions.

The spectral decomposition for two-time (7.20) and temperature (7.23) Green's functions is defined as:

$$\begin{aligned}
G_{r,a}^{AB}(t) &= \frac{1}{2\pi} \int_{-\infty}^{\infty} G_{r,a}^{AB}(\omega) e^{-i\omega t} d\omega, \quad G_{r,a}^{AB}(\omega) = \int_{-\infty}^{\infty} G_{r,a}^{AB}(t) e^{i\omega t} dt, \\
G^{AB}(\tau) &= \Theta \sum_{\omega_n} G^{AB}(\omega_n) e^{-i\omega_n \tau}, \quad G^{AB}(\omega_n) = \frac{1}{2} \int_{-1/\Theta}^{1/\Theta} G^{AB}(\tau) e^{i\omega_n \tau} d\tau, \\
\omega_n &= \begin{cases} 2n\pi \Theta & \text{for Bose particles,} \\ (2n+1)\pi \Theta & \text{for Fermi particles,} \end{cases} \\
n &= 0, \pm 1, \pm 2, \dots
\end{aligned}$$

Green's functions definitions Eq. (7.20), (7.23) leads to relation between the spectral representations of temperature and time Green's functions:

$$G^{AB}(\omega_n) = \begin{cases} G_r^{AB}(i\omega_n/\hbar), & \omega_n > 0, \\ G_a^{AB}(i\omega_n/\hbar), & \omega_n < 0. \end{cases}$$

To obtain Eq. 7.28 we used the above expression.

Accordingly to the indices $(ni\gamma)$ and $(ni\alpha)$ Green's functions of the electrons and phonons subsystems are matrices respectively.

From the motion equations for Green's functions of zero approximation can be obtained [41]:

$$\begin{aligned} G_0^{aa^+}(\varepsilon) &= [\varepsilon - H_0^{(7.1)}]^{-1}, \quad H_0^{(7.1)} = \left\| h_{ni\gamma, n'i'\gamma'}^{(0)} \right\|, \\ G_0^{uu}(\varepsilon) &= [\omega^2 M^{(0)} - \Phi^{(0)}]^{-1}, \quad \Phi^{(0)} = \left\| \Phi_{ni\alpha, n'i'\alpha'}^{(0)} \right\|, \\ M^{(0)} &= \left\| M_i \delta_{nn'} \delta_{ii'} \delta_{\alpha\alpha'} \right\|. \end{aligned} \quad (7.29)$$

Providing that

$$\frac{\left(\frac{\varepsilon^2}{\hbar^2} \Delta M + \Delta \Phi + \Sigma_{phe}(\varepsilon) + \Sigma_{phph}(\varepsilon) \right)_{ni\alpha, n'i'\alpha'}}{\Phi_{ni\alpha, n'i'\alpha'}^{(0)}} \ll 1, \quad (7.30)$$

solution of the system in Eq. 7.28 has the form:

$$\begin{aligned} G^{aa^+}(\varepsilon) &= \left[[G_0^{aa^+}(\varepsilon)]^{-1} - (w + \Sigma_{eph}(\varepsilon) + \Sigma_{ee}(\varepsilon)) \right]^{-1}, \\ G^{uu}(\varepsilon) &= \left[[G_0^{uu}(\varepsilon)]^{-1} - \left(\frac{\varepsilon^2}{\hbar^2} \Delta M + \Delta \Phi + \Sigma_{phe}(\varepsilon) + \Sigma_{phph}(\varepsilon) \right) \right]^{-1}, \\ G^{PP}(\varepsilon) &= \frac{\varepsilon^2}{\hbar^2} (M^{(0)})^2 G^{uu}(\varepsilon), \end{aligned} \quad (7.31)$$

where $\Delta M = \|(M_i - M_{ni})\delta_{nn'}\delta_{ii'}\delta_{\alpha\alpha'}\|$, $\varepsilon = \hbar\omega$.

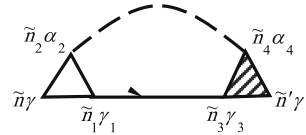
For solution of system in Eq. 7.28 members proportional to the second and higher power of small parameter (7.30) were neglected.

Using the mentioned above diagram technique, in Ref. [28], has been found explicit expressions for the mass operator of Green's functions that describe the many-particle interactions in the system.

The mass operator of Green's function of electrons for the electron-phonon interaction $\Sigma_{eph}(\tau, \tau')$ is described by the diagram in Fig. 7.1.

Solid lines in Fig. 7.1 correspond to the Green's function of electrons $G_{ni\gamma, n'i'\gamma'}^{aa^+}(\tau, \tau')$ and dashed lines correspond to the Green's function of phonons $G_{ni\alpha, n'i'\alpha'}^{uu}(\tau, \tau')$. Vertex part $\Gamma_{ni\gamma, n_1i_1\gamma_1}^{n_2i_2\alpha_2}(\tau_2, \tau, \tau_1)$ is described by diagrams in Fig. 7.2.

Fig. 7.1 Diagram for $\Sigma_{eph, ni\gamma, n'i'\gamma'}(\tau, \tau') = \Sigma_{eph, \tilde{n}\gamma, \tilde{n}'\gamma'}$. Here $\tilde{n} = (ni\tau)$



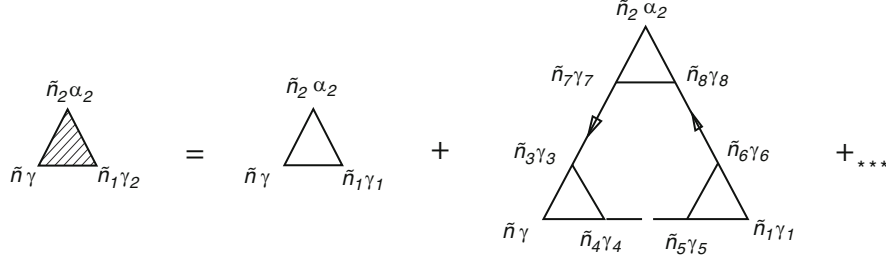
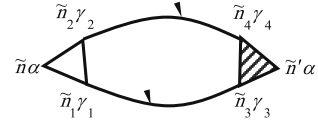


Fig. 7.2 Diagrams for the vertex part $\Gamma_{ni\gamma, n_1 i_1 \gamma_1}^{n_2 i_2 \alpha_2}(\tau_2, \tau, \tau_1) = \Gamma_{\tilde{n}\gamma, \tilde{n}_1 \gamma_1}^{\tilde{n}_2 \alpha_2}$. Here $\tilde{n} = (ni\tau)$

Fig. 7.3 Diagram for $\Sigma_{phe\ n\alpha, n' i' \alpha'}(\tau, \tau') = \Sigma_{phe\ \tilde{n}\alpha, \tilde{n}' \alpha'}$. In Fig. 7.3 $\tilde{n} = (ni\tau)$



No shaded triangle in Fig. 7.2 corresponds to equation

$$\Gamma_{0ni\gamma, n_1 i_1 \gamma_1}^{n_2 i_2 \alpha_2}(\tau_2, \tau, \tau_1) = v_{ni\gamma, n_1 i_1 \gamma_1}^{n_2 i_2 \alpha_2} \delta(\tau - \tau_2) \delta(\tau - \tau_1).$$

In Fig. 7.1 and in Fig. 7.2 summation for internal points $\tilde{n}\gamma$ is carried out. Summation of $\tilde{n}\gamma$ provides summation of $ni\gamma$ and integration over τ . Expressions that correspond instead each diagram attribute multiplier $(-1)^{n+F}$, where n is diagram's order (namely number of vertices Γ_0 in the diagram), and F is the number of lines for the Green's function of electrons G^{aa^+} . This function goes out and goes into in the same vertices.

For the mass operator that describes electron-phonon interaction, we obtained equation

$$\begin{aligned} \Sigma_{eph\ ni\gamma, n' i' \gamma'}(\varepsilon) &= -\frac{1}{4\pi i} \int_{-\infty}^{\infty} d\varepsilon' \coth\left(\frac{\varepsilon'}{2\Theta}\right) v_{ni\gamma, n_3 i_3 \gamma_3}^{m_1 i_1 \alpha_1} \\ &\times [G_{n_1 i_1 \alpha_1, n_2 i_2 \alpha_2}^{uu}(\varepsilon') - G_{n_1 i_1 \alpha_1, n_2 i_2 \alpha_2}^{uu*}(\varepsilon')] G_{n_3 i_3 \gamma_3, n_4 i_4 \gamma_4}^{aa^+} \\ &\times (\varepsilon - \varepsilon') \Gamma_{n_4 i_4 \gamma_4, n' i' \gamma'}^{n_2 i_2 \alpha_2}(\varepsilon - \varepsilon', \varepsilon; \varepsilon'). \end{aligned} \quad (7.32)$$

For repeated indices summation is conducted.

Phonon-electron interaction is described by the diagram in Fig. 7.3.

Designation in Fig. 7.3 corresponds to designations in Figs. 7.1 and 7.2.

Phonon-electron interaction is described by mass operator

$$\begin{aligned} \Sigma_{phenia,n'i'\alpha'}(\varepsilon) &= \frac{1}{2\pi i} \int_{-\infty}^{\infty} d\varepsilon' f(\varepsilon') v_{n_2 i_2 \gamma_2, n_1 i_1 \gamma_1}^{mi\alpha} \\ &\times \left\{ \left[G_{n_1 i_1 \gamma_1, n_3 i_3 \gamma_3}^{aa+}(\varepsilon + \varepsilon') - G_{n_1 i_1 \gamma_1, n_3 i_3 \gamma_3}^{aa+*}(\varepsilon + \varepsilon') \right] \right. \\ &\quad \times G_{n_4 i_4 \gamma_4, n_2 i_2 \gamma_2}^{aa+*}(\varepsilon') + G_{n_1 i_1 \gamma_1, n_3 i_3 \gamma_3}^{aa+}(\varepsilon + \varepsilon') \\ &\quad \left. \times \left[G_{n_4 i_4 \gamma_4, n_2 i_2 \gamma_2}^{aa+}(\varepsilon') - G_{n_4 i_4 \gamma_4, n_2 i_2 \gamma_2}^{aa+*}(\varepsilon') \right] \right\} \\ &\quad \times \Gamma_{n_3 i_3 \gamma_3, n_4 i_4 \gamma_4}^{n'i'\alpha'}(\varepsilon + \varepsilon', \varepsilon; -\varepsilon'). \end{aligned} \quad (7.33)$$

Diagrams for the mass operator $\Sigma_{ee}(\tau, \tau')$ that describes electron-electron interaction, are shown in Fig. 7.4.

Vertex part $\Gamma_{n_2 i_2 \gamma_2, n_1 i_1 \gamma_1}^{n_2 i_2 \gamma_2, n_1 i_1 \gamma_1}(\tau_2, \tau_1, \tau, \tau')$ are shown on diagrams in Fig. 7.5.

Not shaded triangle in Fig. 7.5 corresponds to equation

$$\begin{aligned} \Gamma_{0n_1 i_1 \gamma_1, n' i' \gamma'}^{n_2 i_2 \gamma_2, n_1 i_1 \gamma_1}(\tau_2, \tau_1, \tau, \tau') &= \tilde{v}_{n_1 i_1 \gamma_1, n' i' \gamma'}^{(2)n_1 i_1 \gamma_1, n_2 i_2 \gamma_2} \delta \\ &\quad \times (\tau - \tau_2) \delta(\tau - \tau_1) \delta(\tau - \tau'), \\ \tilde{v}_{n_1 i_1 \gamma_1, n' i' \gamma'}^{(2)n_1 i_1 \gamma_1, n_2 i_2 \gamma_2} &= v_{n_1 i_1 \gamma_1, n' i' \gamma'}^{(2)n_1 i_1 \gamma_1, n_2 i_2 \gamma_2} - v_{n' i' \gamma', n_1 i_1 \gamma_1}^{(2)n_1 i_1 \gamma_1, n_2 i_2 \gamma_2}. \end{aligned}$$

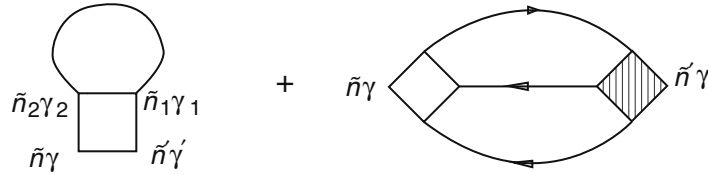


Fig. 7.4 Diagrams for $\Sigma_{ee, n_2 i_2 \gamma_2, n_1 i_1 \gamma_1}(\tau, \tau') = \Sigma_{ee, \tilde{n}_2 \gamma_2, \tilde{n}_1 \gamma_1}$. Here $\tilde{n} = (n\tau)$

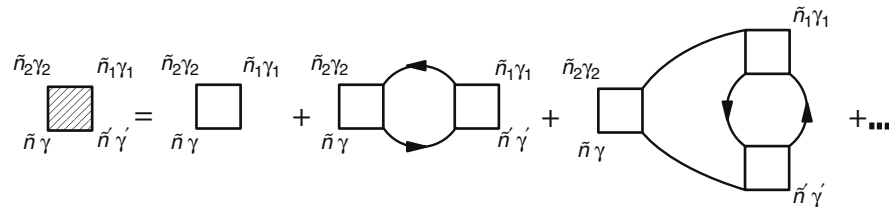


Fig. 7.5 Diagrams for vertex part $\Gamma_{n_2 i_2 \gamma_2, n_1 i_1 \gamma_1}^{n_2 i_2 \gamma_2, n_1 i_1 \gamma_1}(\tau_2, \tau_1, \tau, \tau') = \Gamma_{\tilde{n}_2 \gamma_2, \tilde{n}_1 \gamma_1}^{\tilde{n}_2 \gamma_2, \tilde{n}_1 \gamma_1}$. Here $\tilde{n} = (n\tau)$

The mass operator that describes electron-electron interaction is:

$$\begin{aligned}
\Sigma_{eeniy,n'i'\gamma'}(\varepsilon) &= \Sigma_{eeniy,n'i'\gamma'}^{(1)} + \Sigma_{eeniy,n'i'\gamma'}^{(2)}, \\
\Sigma_{een,n'}^{(1)} &= -\frac{1}{4\pi i} \int_{-\infty}^{\infty} d\varepsilon' f(\varepsilon') \tilde{v}_{n_1,n'}^{(2)n,n_2} \left[G_{n_1,n_2}^{aa+}(\varepsilon') - G_{n_1,n_2}^{aa+*}(\varepsilon') \right], \\
\Sigma_{een,n'}^{(2)}(\varepsilon) &= -\left(\frac{1}{2\pi i} \right)^2 \int_{-\infty}^{\infty} d\varepsilon_1 \int_{-\infty}^{\infty} d\varepsilon_2 \tilde{v}_{n_2,n_1}^{(2)n,n_3} \left\{ f(\varepsilon_1) f(\varepsilon_2) \right. \\
&\times \left[G_{n_2,n_5}^{aa+*}(\varepsilon - \varepsilon_1 + \varepsilon_2) G_{n_1,n_4}^{aa+}(\varepsilon_1) - G_{n_2,n_5}^{aa+}(\varepsilon - \varepsilon_1 + \varepsilon_2) G_{n_1,n_4}^{aa+*}(\varepsilon_1) \right] \\
&\times \left[G_{n_6,n_3}^{aa+}(\varepsilon_2) - G_{n_6,n_3}^{aa+*}(\varepsilon_2) \right] \Gamma_{n_4,n'}^{n_5,n_6}(\varepsilon_1, \varepsilon - \varepsilon_1 + \varepsilon_2; \varepsilon_2, \varepsilon) \\
&\quad \left. + f(\varepsilon_1) f(\varepsilon_1 + \varepsilon_2 - \varepsilon) \left[G_{n_2,n_5}^{aa+}(\varepsilon_2) - G_{n_2,n_5}^{aa+*}(\varepsilon_2) \right] \right. \\
&\times \left[G_{n_1,n_4}^{aa+}(\varepsilon_1) G_{n_6,n_3}^{aa+}(\varepsilon_1 + \varepsilon_2 - \varepsilon) - G_{n_1,n_4}^{aa+*}(\varepsilon_1) G_{n_6,n_3}^{aa+*}(\varepsilon_1 + \varepsilon_2 - \varepsilon) \right] \\
&\quad \left. \times \Gamma_{n_4,n'}^{n_5,n_6}(\varepsilon_1, \varepsilon_2; \varepsilon_1 + \varepsilon_2 - \varepsilon, \varepsilon) \right\}, \tag{7.34}
\end{aligned}$$

$$\tilde{v}_{n_1,n'}^{(7.2)n,n_2} = v_{n_1,n'}^{(7.2)n,n_2} - v_{n',n_1}^{(7.2)n,n_2}, \quad (n \equiv ni\gamma).$$

In Ref. [28] expressions for the mass operator $\Sigma_{phph}(\varepsilon)$ that describe phonon-phonon interaction similarly were obtained.

The relations arising from the theory of functions of complex variable are used upon receipt of expressions (7.32), (7.33) and (7.34).

$$\begin{aligned}
\Theta \sum_{\omega_n} \phi(i\omega_n) &= \frac{1}{4\pi i} \oint_C dz \coth\left(\frac{z}{2\Theta}\right) \phi(z) \quad (\omega_n = 2n\pi\Theta), \\
\Theta \sum_{\omega_n} \phi(i\omega_n) &= -\frac{1}{2\pi i} \oint_C dz f\left(\frac{z}{\Theta}\right) \phi(z) \quad (\omega_n = (2n+1)\pi\Theta), \\
f\left(\frac{z}{\Theta}\right) &= \frac{1}{\exp\left(\frac{z}{\Theta}\right) + 1},
\end{aligned}$$

where $\phi(z)$ is analytic function of complex z in the region covered by a contour C .

Between spectral representations of the Green's functions $G_\mu(\varepsilon)$ defined at constant chemical potential μ_e by Eq.(7.20), and $G_N(\varepsilon)$, defined at a constant number of electrons N_e a relation $G_\mu(\varepsilon) = G_N(\varepsilon + \mu)$ exists.

Renormalization of diagrams vertex parts can be neglected.

$$\begin{aligned}
\Gamma_{n_4 i_4 \gamma_4, n' i' \gamma'}^{\lambda_2 n_2 i_2 \alpha_2}(\varepsilon - \varepsilon', \varepsilon; \varepsilon') &= v_{n_4 i_4 \gamma_4, n' i' \gamma'}^{\lambda_2 n_2 i_2 \alpha_2}, \\
\Gamma_{n_4, n'}^{n_5, n_6}(\varepsilon_1, \varepsilon - \varepsilon_1 + \varepsilon_2; \varepsilon_2, \varepsilon) &= \tilde{v}_{n_6, n'}^{(2)n_4, n_5}.
\end{aligned}$$

In expressions (7.33) and (7.34) $f(\varepsilon)$ is Fermi function. Fermi level $\varepsilon_F \equiv \mu_e$ of system is determined by the equation:

$$\langle Z \rangle = \int_{-\infty}^{\infty} f(\varepsilon, \varepsilon_F) g_e(\varepsilon) d\varepsilon, \quad (7.35)$$

where $\langle Z \rangle$ – average number of electrons per atom, $g_e(\varepsilon)$ – density of electron states.

$$g_e(\varepsilon) = -\frac{1}{\pi \nu N} \text{ImSp} \left\langle G^{aa^+}(\varepsilon) \right\rangle_c. \quad (7.36)$$

In Eq. (7.36) brackets $\langle \dots \rangle_c$ denote configurational averaging, N is a number of primitive cells, ν – number of atoms in the primitive cell. To further reduce of recordings the index c near brackets $\langle \dots \rangle_c$ will be omitted. In the formula (7.35) $\langle Z \rangle$ – average number of electrons per atom.

Equation (7.36) follows from the definition of operator number of electrons in Eq. (7.20) and Green's function $G^{AB}(\tau, \tau')$ (7.23), $A = a_{ni\gamma}^+$, $B = a_{ni\gamma}$.

It should be noted that the first term $\Sigma_{eeni\gamma, n'i'\gamma'}^{(1)}$ in Eq. (7.34) for the mass operator of electron-electron interaction describes the Coulomb and exchange electron-electron interactions in the Hartree–Fock approximation. The second term $\Sigma_{eeni\gamma, n'i'\gamma'}^{(2)}$ which is caused by output beyond the Hartree–Fock approximation, describes the electronic correlation. In contradiction to Refs. [6, 7, 9–11, 14, 26] long-range Coulomb interaction of electrons located at the different sites of the crystal lattice is described taking into account an arbitrary number of energy bands.

Expression in Eq. (7.31) differs from corresponding expressions for the Green's function of the single-particle Hamiltonian of disordered system only by form of mass operators. Therefore to calculate the Green's function given by Eq. (7.31) we use well known methods of the disordered systems theory [28].

7.4 Localized Magnetic Moments

Obtained results give possibilities to investigate the influence of electronic correlations on the electronic structure and properties of the system. To perform this, the heterogeneous distribution of electron density is taken into account. We assume that distribution of electron density corresponds to the minimum of free energy. The mass operator of electron-electron interaction in Eq. (7.34) can be defined through the occupation number $Z_{ni\gamma\sigma}^{\lambda m \lambda_i}$ of electron's states ($ni\gamma\sigma$). The value $Z_{ni\gamma\sigma}^{\lambda m \lambda_i}$ is determined by Eq. (7.35), where density of electronic states $g_e(\varepsilon)$ is replaced by conditional partial density of states $g_{ni\gamma\sigma}^{\lambda m \lambda_i}(\varepsilon)$ for energy band γ and spin projection σ .

The occupation number of electron states $Z_{ni\gamma\sigma}^{\lambda m_{\lambda i}}$ and conditional partial density of states $g_{ni\gamma\sigma}^{\lambda m_{\lambda i}}(\varepsilon)$ are

$$Z_{ni\gamma\sigma}^{\lambda m_{\lambda i}} = \int_{-\infty}^{\infty} f(\varepsilon, \varepsilon_F) g_{ni\gamma\sigma}^{\lambda m_{\lambda i}}(\varepsilon) d\varepsilon,$$

$$g_{ni\gamma\sigma}^{\lambda m_{\lambda i}}(\varepsilon) = -\frac{1}{\pi} \operatorname{Im} \left(G_{ni\gamma\sigma, ni\gamma\sigma}^{aa+}(\varepsilon) \right) \Big|_{(ni) \in \lambda m_{\lambda i}}. \quad (7.37)$$

In the last formula averaging is done along with condition that atom of sort λ is located at the site (ni) , and projection of localized magnetic moment equals to $m_{\lambda i}$. The probability of such event is $P_{ni}^{\lambda m_{\lambda i}}$ and we can write $\sum_{\lambda, m_{\lambda i}} P_{ni}^{\lambda m_{\lambda i}} = 1$.

Thus, we consider the localized magnetic moments which are distributed not homogeneously on the crystal lattice sites (static magnetization fluctuations).

We can also write equations

$$Z_{ni\gamma}^{\lambda m_{\lambda i}} = Z_{ni\gamma\sigma}^{\lambda m_{\lambda i}} + Z_{ni\gamma, -\sigma}^{\lambda m_{\lambda i}}, \quad m_{\lambda i\gamma} = Z_{ni\gamma\sigma}^{\lambda m_{\lambda i}} - Z_{ni\gamma, -\sigma}^{\lambda m_{\lambda i}}. \quad (7.38)$$

From Eq. (7.38) we obtain

$$Z_{ni\gamma\sigma}^{\lambda m_{\lambda i}} = \frac{Z_{ni\gamma}^{\lambda m_{\lambda i}} + m_{\lambda i\gamma}}{2}, \quad Z_{ni\gamma, -\sigma}^{\lambda m_{\lambda i}} = \frac{Z_{ni\gamma}^{\lambda m_{\lambda i}} - m_{\lambda i\gamma}}{2}.$$

Number of electrons and magnetic moment projection for the atom of sort λ at the site (ni) are, respectively:

$$Z_{ni}^{\lambda m_{\lambda i}} = \sum_{\gamma} Z_{ni\gamma}^{\lambda m_{\lambda i}}, \quad m_{\lambda i} = \sum_{\gamma} m_{\lambda i\gamma}.$$

In Eq. (7.31) by introducing the mass operator as the sum of one site operators and selecting as a zero one site approximation of the effective medium Green's function cluster expansion for Green's functions $G^{aa+}(\varepsilon)$, $G^{uu}(\varepsilon)$ is performed. Specified expansion is a generalization of the cluster expansion for the Green's function $G^{aa+}(\varepsilon)$ of single-particle Hamiltonian.

Green's functions in Eq. (7.31) satisfy this equation:

$$G(\varepsilon) = \tilde{G}(\varepsilon) + \tilde{G}(\varepsilon)T(\varepsilon)\tilde{G}(\varepsilon),$$

where T is matrix of scattering and could be represented expansion in series, where which terms describe scattering of the clusters with different numbers of nodes

$$T = \sum_{(n_1 i_1)} t^{n_1 i_1} + \sum_{(n_1 i_1) \neq (n_2 i_2)} T^{(2) n_1 i_1, n_2 i_2} + \dots$$

Here $T^{(2)n_1i_1, n_2i_2} = [I - t^{n_1i_1} \tilde{G} t^{n_2i_2} \tilde{G}]^{-1} t^{n_1i_1} \tilde{G} t^{n_2i_2} [I + \tilde{G} t^{n_1i_1}]$, where $t^{n_1i_1}$ is scattering operator on the same site is determined by equation $t^{n_1i_1} = [I - (\Sigma^{n_1i_1} - \sigma^{n_1i_1}) \tilde{G}]^{-1} (\Sigma^{n_1i_1} - \sigma^{n_1i_1})$. This is $\sigma^{n_1i_1}$ potential of the effective medium (coherent potentials).

By using Eqs. (7.36) and (7.37) and performing averaging over the distribution of atoms of different sort and localized magnetic moments projection at the sites of the crystal lattice and neglecting the contribution of processes of electron scattering in clusters consisting of three or more atoms that are small by the small parameter for the density of electronic states we obtain:

$$\begin{aligned}
g_e(\varepsilon) &= \frac{1}{v} \sum_{i, \gamma, \sigma, \lambda, m_{\lambda i}} P_{0i}^{\lambda m_{\lambda i}} g_{0i\gamma\sigma}^{\lambda m_{\lambda i}}(\varepsilon), \\
g_{0i\gamma\sigma}^{\lambda m_{\lambda i}}(\varepsilon) &= -\frac{1}{\pi} \text{Im} \left\{ \tilde{G} + \tilde{G} t_{0i}^{\lambda m_{\lambda i}} \tilde{G} + \sum_{\substack{(lj) \neq (0i) \\ \lambda', m_{\lambda' j}}} P_{lj 0i}^{\lambda' m_{\lambda' j} / \lambda m_{\lambda i}} \right. \\
&\times \tilde{G} \left[t_{lj}^{\lambda' m_{\lambda' j}} + T^{(2)\lambda m_{\lambda i} 0i, \lambda' m_{\lambda' j} lj} + T^{(2)\lambda' m_{\lambda' j} lj, \lambda m_{\lambda i} 0i} \right] \tilde{G} \left. \right\}^{0i\gamma\sigma, 0i\gamma\sigma}, \\
T^{(2)\lambda m_{\lambda i} 0i, \lambda' m_{\lambda' j} lj} &= \left[I - t^{\lambda m_{\lambda i} 0i} \tilde{G} t^{\lambda' m_{\lambda' j} lj} \tilde{G} \right]^{-1} \\
&\times t^{\lambda m_{\lambda i} 0i} \tilde{G} t^{\lambda' m_{\lambda' j} lj} [I + \tilde{G} t^{\lambda m_{\lambda i} 0i}], \tag{7.39}
\end{aligned}$$

where $\tilde{G} = \tilde{G}^{aa^\dagger}(\varepsilon)$.

Energy spectrum calculation is done by iterative procedure. The first step of iterative procedure is described above.

On the next steps of iterative procedure values of occupation number of electron basis states in Eq. (7.14) is calculated by expression:

$$Z_{i\delta\sigma}^\lambda = \frac{1}{2} (Z_{i\delta c\sigma}^\lambda + Z_{i\delta s\sigma}^\lambda), \tag{7.40}$$

where $Z_{i\delta c\sigma}^\lambda, Z_{i\delta s\sigma}^\lambda$ defined by expression (7.37) for $Z_{ni\gamma\sigma}^{\lambda m_{\lambda i}}$, $\gamma = (\delta c), (\delta s)$ and $\delta = (\tilde{e}lm)$. Expression (7.40) obtained using Eq. (7.16).

Above mentioned procedure of energy spectrum calculation is self-consistent.

7.5 Free Energy

Thermodynamic potential of the system is

$$\Omega = -\Theta \ln \text{Sp}(e^{-H/\Theta}).$$

Free energy F as a function of volume V , temperature T , number of electrons N_e and parameters of interatomic correlations $(\varepsilon_{n_1 i_1, n_2 i_2}, \eta)$ to the thermodynamic potential Ω is expressed via expression $F = \Omega + \mu_e \langle N_e \rangle$. Free energy F in the weak dependence of the mass operators on the energy of electrons and phonon approximation can be represented in the form [17–19, 28]

$$F = \langle \delta \Phi \rangle - \Theta S_c + \Omega_e + \Omega_{ph} + \mu_e \langle Z \rangle, \quad (7.41)$$

where Ω_e, Ω_{ph} are given by

$$\Omega_e = -\Theta \int_{-\infty}^{\infty} \ln(1 + e^{(\mu_e - \varepsilon)/\Theta}) g_e(\varepsilon) d\varepsilon,$$

$\Omega_{ph} = \Theta \int_{-\infty}^{\infty} \ln(1 - e^{-\varepsilon/\Theta}) g_{ph}(\varepsilon) d\varepsilon$ – the thermodynamic potential of atomic nucleus in field of ionic cores.

In Eq. (7.41) the values $F, S_c, \Omega_e, \Omega_{ph}$ are calculated per one atom.

7.6 Electrical Conductivity

For electrical conductivity tensor calculation Kubo's formula is used [20]

$$\sigma_{\alpha\beta}(\omega) = \int_0^{1/\Theta} \int_0^{\infty} e^{i\omega t - \delta t} \langle \tilde{J}_\beta(0) \tilde{J}_\alpha(t + i\hbar\tau) \rangle d\tau dt, \quad (7.42)$$

where J_α is the operator of the α is projection of the current density.

From Eq. (7.42) it follows:

$$\text{Re } \sigma_{\alpha\beta}(\omega) = \frac{i}{2\omega} \left[G_r^{J_\alpha J_\beta}(\omega) - G_a^{J_\alpha J_\beta}(\omega) \right].$$

To calculate the spectral representations $G_r^{J_\alpha J_\beta}(\omega)$ and $G_a^{J_\alpha J_\beta}(\omega)$ of the retarded and the advanced Green's functions the expression for current-density operator is used

$$J_\alpha(t) = e \int \Psi^+(\xi, t) v_\alpha \Psi(\xi, t) d\xi,$$

where $\Psi^+(\xi, t)$ and $\Psi(\xi, t)$ are field operators of electron's creation and annihilation respectively; v_α is the operator of the α – projection of the velocity; e is the electron charge; by integrating over ξ we mean integrating over the crystal volume and summing over the projection of spin σ onto the z axis; and the crystal's volume is assumed to be equal to unity.

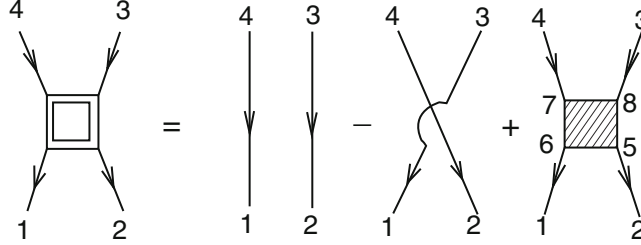


Fig. 7.6 Diagrams for the two-particle Green's function

In this case the temperature Green's function is

$$G^{J\alpha J\beta}(\tau, \tau') = \frac{e^2}{NV_1} \sum_{n_1 n_2 n_3 n_4} v_{\alpha n_4 n_2} v_{\beta n_3 n_1} G''(n_1 \tau', n_2 \tau, n_3 \tau', n_4 \tau),$$

where V_1 – volume of primitive cell, the two-particle Green's function is

$$\begin{aligned} & G''(n_1 \tau', n_2 \tau, n_3 \tau', n_4 \tau) \\ &= \langle T_{\tau} a_{n_1}(\tau') a_{n_2}(\tau) a_{n_3}^+(\tau') a_{n_4}^+(\tau) \sigma(1/\theta) \rangle_0 \langle \sigma(1/\theta) \rangle_0^{-1}, \\ & \quad (n = ni\gamma). \end{aligned}$$

The two-particle Green's function is described by the diagram in Fig. 7.6. Numbers of Fig. 7.6 correspond to point numbers, e.g., 1 corresponds to $(n_1 i_1 \gamma_1 \tau_1)$.

Using the diagram technique for two-particle temperature Green's function and neglecting the contributions of scattering processes on clusters of three or more sites for the static conductivity tensor we can get

$$\begin{aligned} \sigma_{\alpha\beta} &= \frac{e^2 \hbar}{4\pi V_1} \left\{ \int_{-\infty}^{\infty} d\varepsilon_1 \frac{\partial f}{\partial \varepsilon_1} \sum_{s, s' = +, -} (2\delta_{ss'} - 1) \sum_{\sigma\gamma, i} \left\{ [v_{\beta} \tilde{K}(\varepsilon_1^s, v_{\alpha}, \varepsilon_1^{s'})] \right. \right. \\ &+ \sum_{\lambda, m_{\lambda i}} P_{0i}^{\lambda m_{\lambda i}} \tilde{K}(\varepsilon_1^s, v_{\beta}, \varepsilon_1^s) (t_{0i}^{\lambda m_{\lambda i}}(\varepsilon_1^s) \tilde{K}(\varepsilon_1^s, v_{\alpha}, \varepsilon_1^{s'}) t_{0i}^{\lambda m_{\lambda i}}(\varepsilon_1^{s'})) \\ &+ \sum_{\lambda, m_{\lambda i}} P_{0i}^{\lambda m_{\lambda i}} \sum_{\substack{l_j \neq 0i \\ \lambda', m_{\lambda' j}}} P_{l_j 0i}^{\lambda' m_{\lambda' j} / \lambda m_{\lambda i}} \left[[\tilde{K}(\varepsilon_1^s, v_{\beta}, \varepsilon_1^s) v_{\alpha} \tilde{G}(\varepsilon_1^{s'})] \right. \\ &\quad \times T^{(2)\lambda m_{\lambda i} 0i, \lambda' m_{\lambda' j} l_j}(\varepsilon_1^{s'}) \\ &\quad + [\tilde{K}(\varepsilon_1^s, v_{\beta}, \varepsilon_1^s) v_{\alpha} \tilde{G}(\varepsilon_1^{s'})] T^{(2)\lambda' m_{\lambda' j} l_j, \lambda m_{\lambda i} 0i}(\varepsilon_1^{s'}) \\ &\quad \left. \left. + [\tilde{K}(\varepsilon_1^s, v_{\alpha}, \varepsilon_1^{s'}) v_{\beta} \tilde{G}(\varepsilon_1^s)] T^{(2)\lambda m_{\lambda i} 0i, \lambda' m_{\lambda' j} l_j}(\varepsilon_1^s) \right\} \right\} \end{aligned}$$

$$\begin{aligned}
& + [\tilde{K}(\varepsilon_1^s, v_\alpha, \varepsilon_1^{s'}) v_\beta \tilde{G}(\varepsilon_1^s)] T^{(2)\lambda' m_{\lambda' j l j, \lambda m_{\lambda i} 0 i}(\varepsilon_1^s)} \\
& + \tilde{K}(\varepsilon_1^{s'}, v_\beta, \varepsilon_1^s) \left[(t_{ij}^{\lambda' m_{\lambda' j}}(\varepsilon_1^s) \tilde{K}(\varepsilon_1^s, v_\alpha, \varepsilon_1^{s'}) t_{0i}^{\lambda m_{\lambda i}}(\varepsilon_1^{s'}) \right. \\
& + t_{ij}^{\lambda' m_{\lambda' j}}(\varepsilon_1^s) \tilde{K}(\varepsilon_1^s, v_\alpha, \varepsilon_1^{s'}) T^{(2)\lambda m_{\lambda i} 0 i, \lambda' m_{\lambda' j l j}(\varepsilon_1^{s'})} \\
& + T^{(2)\lambda' m_{\lambda' j l j, \lambda m_{\lambda i} 0 i}(\varepsilon_1^s) \tilde{K}(\varepsilon_1^s, v_\alpha, \varepsilon_1^{s'}) t_{0i}^{\lambda m_{\lambda i}}(\varepsilon_1^{s'}) \\
& \left. + T^{(2)\lambda' m_{\lambda' j l j, \lambda m_{\lambda i} 0 i}(\varepsilon_1^s) \tilde{K}(\varepsilon_1^s, v_\alpha, \varepsilon_1^{s'}) T^{(2)\lambda m_{\lambda i} 0 i, \lambda' m_{\lambda' j l j}(\varepsilon_1^{s'})} \right] \left. \right\}^{0i\gamma\sigma, 0i\gamma\sigma} \\
& + \int_{-\infty}^{\infty} \int_{-\infty}^{\infty} d\varepsilon_1 d\varepsilon_2 f(\varepsilon_1) f(\varepsilon_2) \left\langle \Delta G_{\alpha\beta}^{II}(\varepsilon_1, \varepsilon_2) \right\rangle, \tag{7.43}
\end{aligned}$$

where

$$\begin{aligned}
\tilde{K}(\varepsilon_1^s, v_\alpha, \varepsilon_1^{s'}) &= \tilde{G}^{aa^+}(\varepsilon_1^s) v_\alpha \tilde{G}^{aa^+}(\varepsilon_1^{s'}), \\
\tilde{G}^{aa^+}(\varepsilon_1^+) &= \tilde{G}_r^{aa^+}(\varepsilon_1), \\
\tilde{G}^{aa^+}(\varepsilon_1^-) &= \tilde{G}_a^{aa^+}(\varepsilon_1) = \left(\tilde{G}_r^{aa^+} \right)^*(\varepsilon_1).
\end{aligned}$$

In Eq. (7.43) component of two-particle Green's function $\Delta G_{\alpha\beta}^{II}(\varepsilon_1, \varepsilon_2)$ is caused by the interaction and has the form:

$$\begin{aligned}
\Delta G_{\alpha\beta}^{II}(\varepsilon_1, \varepsilon_2) &= \frac{i}{2\pi} v_{\alpha n_4 n_2} v_{\beta n_3 n_1} \left\{ \left[G_{m_1 n_6}^{aa^+}(\varepsilon_1) - G_{a n_1 n_6}^{aa^+}(\varepsilon_1) \right] \right. \\
& \times \left[G_{m_2 n_5}^{aa^+}(\varepsilon_2) - G_{a n_2 n_5}^{aa^+}(\varepsilon_2) \right] \left[G_{a n_7 n_4}^{aa^+}(\varepsilon_2) G_{m_8 n_3}^{aa^+}(\varepsilon_1) \right. \\
& - G_{m_7 n_4}^{aa^+}(\varepsilon_2) G_{a n_8 n_3}^{aa^+}(\varepsilon_1) \left. \right] + G_{a n_1 n_6}^{aa^+}(\varepsilon_1) \left[G_{m_2 n_5}^{aa^+}(\varepsilon_2) - G_{a n_2 n_5}^{aa^+}(\varepsilon_2) \right] \\
& \times G_{a n_7 n_4}^{aa^+}(\varepsilon_2) \left[G_{m_8 n_3}^{aa^+}(\varepsilon_1) - G_{a n_8 n_3}^{aa^+}(\varepsilon_1) \right] - G_{m_1 n_6}^{aa^+}(\varepsilon_1) \\
& \times \left[G_{m_2 n_5}^{aa^+}(\varepsilon_2) - G_{a n_2 n_5}^{aa^+}(\varepsilon_2) \right] G_{m_7 n_4}^{aa^+}(\varepsilon_2) \left[G_{m_8 n_3}^{aa^+}(\varepsilon_1) - G_{a n_8 n_3}^{aa^+}(\varepsilon_1) \right] \\
& + \left[G_{a n_1 n_6}^{aa^+}(\varepsilon_1) G_{m_2 n_5}^{aa^+}(\varepsilon_2) - G_{m_1 n_6}^{aa^+}(\varepsilon_1) G_{a n_2 n_5}^{aa^+}(\varepsilon_2) \right] \\
& \times \left[G_{m_7 n_4}^{aa^+}(\varepsilon_2) - G_{a n_7 n_4}^{aa^+}(\varepsilon_2) \right] \left[G_{m_8 n_3}^{aa^+}(\varepsilon_1) - G_{a n_8 n_3}^{aa^+}(\varepsilon_1) \right] \\
& \left. + \left[G_{m_1 n_6}^{aa^+}(\varepsilon_1) - G_{a n_1 n_6}^{aa^+}(\varepsilon_1) \right] G_{m_2 n_5}^{aa^+}(\varepsilon_2) \left[G_{m_7 n_4}^{aa^+}(\varepsilon_2) - G_{a n_7 n_4}^{aa^+}(\varepsilon_2) \right] \right\}
\end{aligned}$$

$$\begin{aligned}
& + \left[G_{m_1 n_6}^{aa^+}(\varepsilon_1) - G_{an_1 n_6}^{aa^+}(\varepsilon_1) \right] G_{m_2 n_5}^{aa^+}(\varepsilon_2) \left[G_{m_7 n_4}^{aa^+}(\varepsilon_2) - G_{an_7 n_4}^{aa^+}(\varepsilon_2) \right] \\
& \quad \times G_{m_8 n_3}^{aa^+}(\varepsilon_1) - \left[G_{m_1 n_6}^{aa^+}(\varepsilon_1) - G_{an_1 n_6}^{aa^+}(\varepsilon_1) \right] G_{an_2 n_5}^{aa^+}(\varepsilon_2) \\
& \quad \times \left[G_{m_7 n_4}^{aa^+}(\varepsilon_2) - G_{an_7 n_4}^{aa^+}(\varepsilon_2) \right] G_{an_8 n_3}^{aa^+}(\varepsilon_1) \left. \vphantom{G_{m_1 n_6}^{aa^+}} \right\} \Gamma_{n_5 n_8}^{n_6 n_7}(\varepsilon_1, \varepsilon_2; \varepsilon_2, \varepsilon_1) \quad (7.44)
\end{aligned}$$

($n \equiv ni\gamma\sigma$).

Operator α -projection of the electron velocity in Eq. (7.43) is:

$$v_\alpha(\mathbf{k}) = \frac{1}{\hbar} \frac{\partial H_0^{(1)}(k)}{\partial k_\alpha}.$$

To simplify the formula (7.44) we use approximate expression $\langle \Delta G_{\alpha\beta}^H(\varepsilon_1; \varepsilon_2) \rangle \approx \Delta \tilde{G}_{\alpha\beta}^H(\varepsilon_1; \varepsilon_2)$, where $\Delta \tilde{G}_{\alpha\beta}^H(\varepsilon_1; \varepsilon_2)$ is derived from the Eq. (7.43) by replacing the $G^{aa^+}(\varepsilon)$ with $\tilde{G}^{aa^+}(\varepsilon)$.

7.7 Spin-Dependent Transport of Carbon Nanotubes with Chromium Atoms

In this section the results of calculation of the energy spectrum of electrons and phonons and conductivity of carbon nanotubes doped with chromium are represented. Renormalization of vertex parts diagrams for the mass operators in Eqs. (7.32), (7.33) and (7.34) and contribution of the static displacements of atoms in the calculations are neglected. The contribution of matrix elements on the basis of real wave functions $v_{n_3 i_3 \gamma_3, n_4 i_4 \gamma_4}^{(2) n_1 i_1 \gamma_1, n_2 i_2 \gamma_2}$ in Eq. (7.34) for different sites (ni) is neglected. As the basis $2s$, $2p$ -states wave functions of the neutral carbon atoms and $3d$, $4s$ -states wave functions of the neutral chromium atoms were chosen. The initial ion core's valence of C and Cr atoms Z^{λ_i} are 4 and 6 respectively. To simplify calculations in the above-mentioned self-consistent iterative procedure was performed only first step. In expression (7.14) $Z_{i\delta\sigma}^\lambda = 1$ for occupied electronic states. The off-diagonal matrix elements (ni) by site index of Hamiltonian in Eq. (7.1) were calculated by taking into account the first three coordination spheres. For Green function calculation 10^3 points for Brillouin zone are used. For mass operator calculation in Eqs. (7.32), (7.33) and (7.34) numerical integration is applied. Calculations were performed for the temperature $T = 300$ K.

We performed geometry optimization of the crystal structure of carbon nanotube with (3, 0) chirality doped by Cr atoms. Geometric optimization of the crystal structure was achieved by minimization the free energy F , defined in Eq. (7.41). Carbon nanotube doped with Cr has a one-dimensional crystal structure. Primitive cell contains 18 non-equivalent atom positions. Carbon atoms are located in 12

Fig. 7.7 The crystal structure of carbon nanotube with (3,0) chirality doped by Cr atoms. The top view. *Black* – C atoms, *white* – Cr atoms

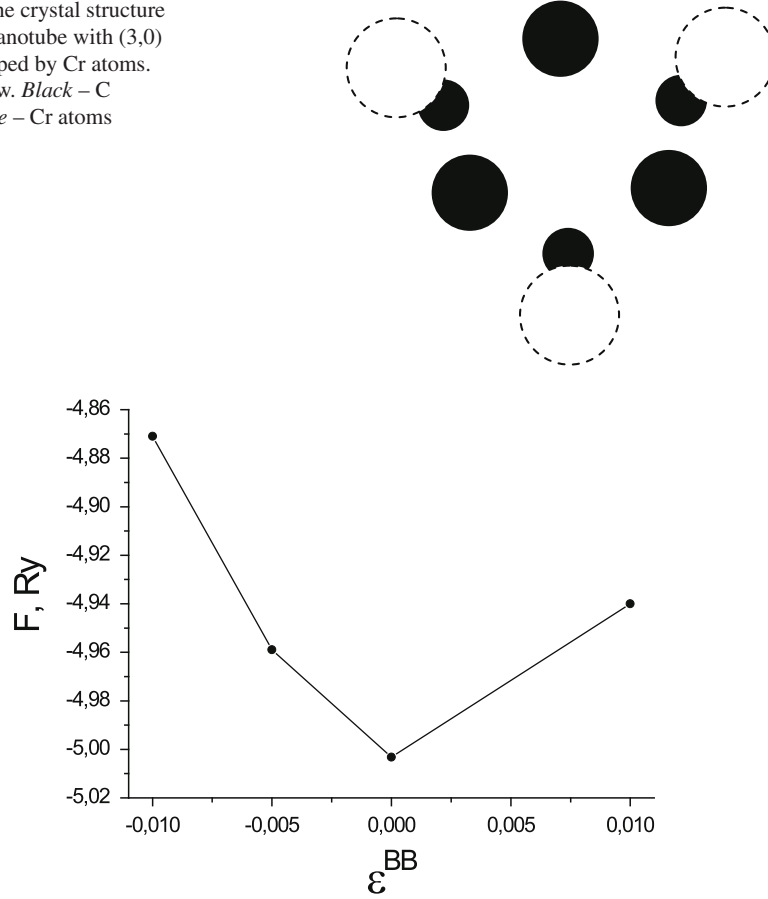


Fig. 7.8 Dependence of free energy F for carbon nanotubes with 5 atoms of Cr per primitive cell on parameter of pair correlations in the arrangement of Cr impurities on lattice sites ε^{BB}

positions on the surface of the inner cylinder. The distance between the carbon atoms is 0.142 nm. Cr atoms are located in 6 positions on the outer surface of the cylinder opposite the center of a hexagon, the vertices of which are carbon atoms. The distance between carbon atoms and Cr is 0.22 nm. The crystal structure of carbon nanotube with (3,0) chirality with Cr impurity is showed at Fig. 7.7.

Through the study of free energy minimum found that Cr atoms are randomly located on the surface of nanotubes. In Fig. 7.8 points shows the dependence of the free energy F in Eq. (7.41) on the parameter of pair correlations in the arrangement of Cr impurities on lattice sites $\varepsilon^{BB} = \varepsilon_{j0i}^{BB}$ in Eq. (7.33) for the first coordination sphere. Atom of Cr is denoted as atom of sort B . The dependence $F(\varepsilon^{BB})$ is shown in the region of free energy minimum.

As shown in Fig. 7.8, the free energy F minimum corresponds to $\varepsilon^{BB} = 0$. This is a result of Cr atoms are randomly located on the surface of carbon nanotube.

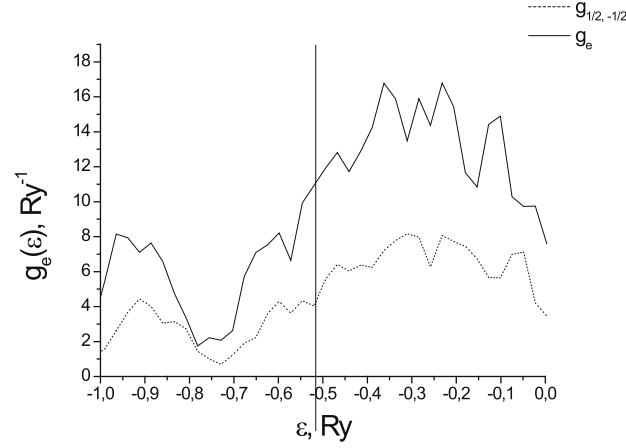


Fig. 7.9 Densities of electron states of carbon nanotube with an admixture of Cr

The relative position of carbon atoms and Cr is similar to the location of atoms of transition metals on the surface of carbon nanotubes of large diameter, which are described in Ref. [39, 40] by ultrasoft pseudopotential method.

The value of localized magnetic moment projection of the atom Cr and induced localized magnetic moment of an atom C in the direction of the magnetic field increases with the size of the field. For carbon nanotubes of 5 Cr atoms in primitive cell value of projection of magnetic moment of the atom Cr varies within $m_{Cr} = (1.02; 2, 24)\mu_B$, and the magnetic moment of the atom C – within $m_C = (0, 0036; 0, 02)\mu_B$ with increasing values of the magnetic field from zero to $H = 200$ A/m. The magnetic field is oriented along the axis of the carbon nanotube. Parameter of pair correlations in the orientation of localized magnetic moments on lattice sites for the first coordination sphere in the absence of magnetic field equals to $\varepsilon^m = 0.235$. The value ε^m for the second and third coordination spheres are close to zero. A positive value of ε^m for the first coordination sphere indicates that the localized magnetic moment given carbon atom is oriented in the same direction as the magnetic moment of the nearest Cr atom.

Figure 7.9 shows a partial $g_{e\sigma}(\varepsilon) = \frac{1}{v} \sum_{i,\gamma,\lambda} P_{0i}^\lambda g_{0i\gamma\sigma}^\lambda(\varepsilon)$ and full $g_e(\varepsilon) = \sum_{\sigma} g_{e\sigma}(\varepsilon)$ densities of electron states of carbon nanotube with an admixture of Cr in the absence of external magnetic field calculated by Eq. (7.32). In the absence of a magnetic field $g_{1/2}(\varepsilon) = g_{-1/2}(\varepsilon)$. Vertical line shows the Fermi level ε_F .

Figure 7.10 shows partial $g_{e\sigma}(\varepsilon)$ and full $g_e(\varepsilon)$ densities of electron states of carbon nanotube with 5 atoms of Cr per primitive cell in external magnetic field $H = 100$ A/m.

In Fig. 7.10 the part of energy spectrum that is close to the Fermi level is showed.

As shown in Fig. 7.10, line of partial $g_{e\sigma}(\varepsilon)$ density of electron states for spin $\sigma = 1/2$ is shifted relative to line for spin $\sigma = -1/2$. The results presented in Fig. 7.10, are qualitatively consistent with results obtained by another method

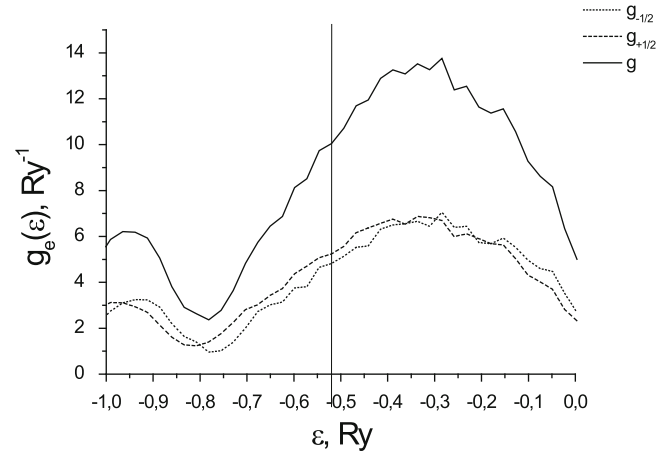


Fig. 7.10 Densities of electron states of carbon nanotube with 5 atoms of Cr per primitive cell in external magnetic field $H = 100$ A/m

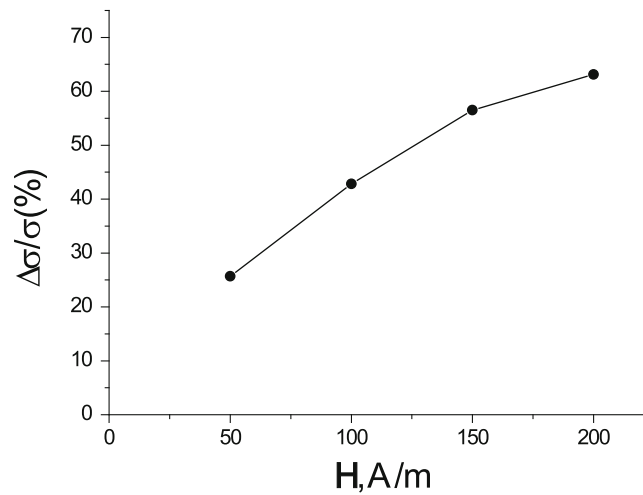


Fig. 7.11 The dependence of spin polarized electric current $\Delta\sigma/\sigma$ of carbon nanotube on the magnitude of the external magnetic field H

in Ref. [39]. In contradiction to our research in Ref. [39] carbon nanotubes with (9;0) chirality doped by Co atoms located inside of the nanotube were described. Quantitative differences in results derived in our research and results of Ref. [39] are determined by this.

In Fig. 7.11 the dependence of the spin polarization electric current $\Delta\sigma/\sigma = (\sigma_{1/2} - \sigma_{-1/2})$ of carbon nanotube with chirality (3.0) and 5 atoms of Cr per primitive cell on the magnitude of the external magnetic field calculated by Eq. (7.43) for temperature 300 K is shown.

7.8 Conclusion

The previously mentioned methods [4, 6, 7, 9–11, 14, 23–26, 30, 35, 36, 38] are used only for the description of ideal ordered crystals and molecules. However, a new method of describing electronic correlations in disordered magnetic crystals based on the Hamiltonian of multi-electron system and diagram method for finding Green's functions is developed.

The nature of spin-dependent electron transport of carbon nanotubes with chromium atoms, which were adsorbed on the surface was found. The phenomenon of spin-dependent electron transport in a carbon nanotube is the result of strong electron correlations caused by the presence of chromium atoms. The value of the spin polarization of electron transport in carbon nanotubes with chromium atoms, which were adsorbed on the surface, is determined by the difference of the partial densities of electron's states (see Fig. 7.10) with opposite spin projection at the Fermi level. This value is also determined by the difference between the relaxation times which arise from different occupation numbers of single-electron states $Z_{n_i i_j \gamma \sigma}^\lambda$ of atoms of carbon and chromium [see Eq. (54)]. The spin polarization of the electric current value increases with Cr atoms concentration and magnitude of the external magnetic field increase. The electronic structure and properties of carbon nanotubes with transition metal chains, adsorbed on the surface, based on the density functional method [23–25, 35, 36] using ultra-soft pseudopotential was calculated [5]. Our results are qualitatively consistent with the results of Ref. [5]. In this paper electron density functional method showed that the chains of transition metals adsorbed on the surface of carbon nanotubes. They open a gap in the electrons states with a certain spin value. Contradictory to Ref.[5] it is shown that atoms of Cr are randomly placed on the carbon nanotube surface.

References

1. Abrikosov AA, Gorkov LP, Dzyaloshinski IE (1963) *Methods of quantum field theory in statistical physics* (edited by Silverman RA). Prentice-Hall, Englewood Cliffs
2. Blochl PE (1994) Projector augmented-wave method. *Phys Rev B* 50:17953
3. Chepulsii RV, Butler WH (2005) Temperature and particle-size dependence of the equilibrium order parameter of FePt alloys. *Phys Rev B* 72:134205
4. Ducastelle F (1974) Derivation of the coherent potential approximation from the atomic limit in the disordered alloy problem. *J Phys C* 7:1795
5. Durgun E, Ciraci S (2006) Spin-dependent electronic structure of transition-metal atomic chains adsorbed on single-wall carbon nanotubes. *Phys Rev B* 74:125404
6. Elstner M, Porezag D, Jungnickel G, Elsner J, Haugk M, Frauenheim T, Suhai S, Seifert G (1998) Self-consistent-charge density-functional tight-binding method for simulations of complex materials properties. *Phys Rev B* 58:7260
7. Enyaschin A, Gemming S, Heine T, Seifert G, Zhechkov L (2006) C₂₈ fullerites-structure, electronic properties and intercalates. *Phys Chem Chem Phys* 8:3320
8. Harrison WA (1966) *Pseudopotentials in the theory of metals*. Benjamin, New York

9. Ivanovskaya VV, Seifert G (2004) Tubular structures of titanium disulfide TiS_2 . *Solid State Commun* 130:175
10. Ivanovskaya VV, Heine T, Gemming S, Seifert G (2006) Structure, stability and electronic properties of composite $\text{Mo}_{1-x}\text{Nb}_x\text{S}_2$ nanotubes. *Phys Status Solidi B* 243:1757
11. Ivanovskaya VV, Köhler C, Seifert G (2007) 3d metal nanowires and clusters inside carbon nanotubes: structural, electronic, and magnetic properties. *Phys Rev B* 75:075410
12. Johnson DD, Nicholson DM, Pinski FJ, Gyorffy BL, Stocks GM (1990) Total-energy and pressure calculations for random substitutional alloys. *Phys Rev B* 41:9701
13. Jones RO, Gunnarsson O (1989) The density functional formalism, its applications and prospects. *Rev Mod Phys* 61:689
14. Köhler C, Seifert G, Gerstmann U, Elstner M, Overhof H, Frauenheim T (2001) Approximate density-functional calculations of spin densities in large molecular systems and complex solids. *Phys Chem Chem Phys* 3:5109
15. Kohn W, Sham LJ (1965) Self-consistent equations Including exchange and correlation effects. *Phys Rev* 140:A1133
16. Kresse G, Joubert D (1999) From ultrasoft pseudopotentials to the projector augmented-wave method. *Phys Rev B* 59:1758
17. Kruchinin SP (1995) Functional integral of antiferromagnetic spin fluctuations in high-temperature superconductors. *Modern Phys Lett B* 9:205–215
18. Kruchinin SP (2014) Physics of high-Tc superconductors. *Rev Theor Phys* 2:124–145
19. Kruchinin S, Nagao H, Aono S (2010) Modern aspects of superconductivity: theory of Superconductivity. World Scientific, Singapore, p 220
20. Kubo R (1957) Statistical-mechanical theory of irreversible processes. 1. General theory and simple applications to magnetic and conduction problems. *J Phys Soc Jpn* 12:570
21. Laasonen K, Car R, Lee C, Vanderbilt D (1991) Implementation of ultrasoft pseudopotentials in ab initio molecular dynamics. *Phys Rev B* 43:6796
22. Los' VF, Repetsky SP (1994) A theory for the electrical conductivity of an ordered alloy. *J Phys Condens Matter* 6:1707
23. Perdew JP, Burke K, Ernzerhof M (1996) Generalized gradient approximation made simple. *Phys Rev Lett* 77:3865
24. Perdew JP, Kurth S, Zupan A, Blaha P (1999) Accurate density functional with correct formal properties: a step beyond the generalized gradient approximation. *Phys Rev Lett* 82:2544
25. Perdew JP, Ruzsinszky A, Csonka GI, Constantin LA, Sun J (2009) Workhorse semilocal density functional for condensed matter physics and quantum chemistry. *Phys Rev Lett* 103:026403
26. Porezag D, Frauenheim T, Köhler T, Seifert G, Kascher R (1995) Construction of tight-binding-like potentials on the basis of density-functional theory: application to carbon. *Phys Rev B* 51:2947
27. Razei SSA, Staunton JB, Ginatempo B, Bruno E, Pinski FJ (2001) The effects of magnetic annealing of transition metal alloys deduced from ab initio electronic structure calculations. *J Phys: Condens Matter* 13:8565
28. Repetsky SP, Shatnii TD (2002) *Theor Math Phys* 131:456
29. Sharma RR (1979) General expressions for reducing the Slater-Koster linear combination of atomic orbitals integrals to the two-center approximation. *Phys Rev B* 19:2813
30. Slater JC (1963) Quantum theory of molecules and solids: electronic structure of molecules, vol 1. McGraw-Hill, New York
31. Slater JC, Koster GF (1954) Simplified LCAO method for the periodic potential problem. *Phys Rev* 94:1498
32. Staunton JB, Razei SSA, Ling MF, Johnson DD, Pinski FJ (1998) Magnetic alloys, their electronic structure and micromagnetic and microstructural models. *J Phys D: Appl Phys* 31:2355
33. Stocks GM, Winter H (1982) Self-consistent-field-Korringa-Kohn-Rostoker-coherent-potential approximation for random alloys. *Z Phys B* 46:95

34. Stocks GM, Temmerman WM, Gyorffy BL (1978) Complete solution of the Korringa-Kohn-Rostoker coherent-potential-approximation equations: Cu-Ni alloys. *Phys Rev Lett* 41:339
35. Sun J, Marsman M, Csonka GI, Ruzsinszky A, Hao P, Kim Y-S, Kresse G, Perdew JP (2011) Self-consistent meta-generalized gradient approximation within the projector-augmented-wave method. *Phys Rev B* 84:035117
36. Tao J, Perdew JP, Staroverov VN, Scuseria GE (2003) Climbing the density functional ladder: nonempirical meta-generalized gradient approximation designed for molecules and solids. *Phys Rev Lett* 91:146401
37. Vanderbilt D (1985) Soft self-consistent pseudopotentials in a generalized eigenvalue formalism. *Phys Rev B* 41:7892
38. Wigner EP (1959) *Group theory*. Academic Press, New York/London
39. Yang C, Zhao J, Lu JP (2003) Magnetism of transition-metal/carbon-nanotube hybrid structures. *Phys Rev Lett* 90:257203
40. Yang C, Zhao J, Lu JP (2004) Complete spin polarization for a carbon nanotube with an adsorbed atomic transition-metal chain. *Nano Lett* 4:561
41. Zubarev DN (1974) *Nonequilibrium statistical thermodynamics* (edited by Gray P, Shepherd PJ). Consultants Bureau, New York